Neuro-Oncology

Neuro-Oncology 18(4), 518–527, 2016
doi:10.1093/neuonc/nov173
Advance Access date 26 September 2015

Combination viroimmunotherapy with checkpoint inhibition to treat glioma, based on location-specific tumor profiling

Julia V. Cockle†, Karishma Rajani†, Shane Zaidi, Timothy Kottke, Jill Thompson, Rosa Maria Diaz, Kevin Shim, Tim Peterson, Ian F. Parney, Susan Short, Peter Selby, Elizabeth Ilett, Alan Melcher, and Richard Vile

Leeds Institute of Cancer Studies and Pathology, University of Leeds, Leeds, UK (J.V.C., S.S., P.S., E.I., A.M., R.V.); Department of Immunology, Mayo Clinic, Rochester, Minnesota (K.R., S.Z., T.K., J.T., R.M.D., K.S., R.V.); Division of Cancer Biology, The Institute of Cancer Research, Chester Beatty Laboratories, London, UK (S.Z., R.V.); Department of Neurologic Surgery, Mayo Clinic, Rochester, Minnesota (T.P., I.F.P.)

Corresponding Author: Richard Vile, PhD, Mayo Clinic, Gugg 18, 200 First Street SW, Rochester, MN 55905 (vile.richard@mayo.edu).

†These authors contributed equally to this work.

Background. Systemic delivery of a complementary cDNA library expressed from the vesicular stomatitis virus (VSV) treats tumors by vaccinating against a wide range of tumor associated antigens (TAAs). For subcutaneous B16 melanomas, therapy was achieved using a specific combination of self-TAAs (neuroblastoma-Ras, cytochrome *c*, and tyrosinase-related protein 1) expressed from VSV. However, for intracranial B16 tumors, a different combination was therapeutic (consisting of VSV-expressed hypoxia-inducible factor [HIF]–2α, Sox-10, c-Myc, and tyrosinase-related protein 1). Therefore, we tested the hypothesis that tumors of different histological types growing in the brain share a common immunogenic signature which can be exploited for immunotherapy.

Methods. Syngeneic tumors, including GL261 gliomas, in the brains of immune competent mice were analyzed for their antigenic profiles or were treated with systemic viroimmunotherapy.

Results. Several different histological types of tumors growing intracranially, as well as freshly resected human brain tumor explants, expressed a HIF-2α^{Hi} phenotype imposed by brain-derived CD11b+ cells. This location-specific antigen expression was exploited therapeutically against intracranial GL261 gliomas using systemically delivered VSV expressing HIF-2α, Sox-10, and c-Myc. Viroimmunotherapy was enhanced by immune checkpoint inhibitors, associated with the de-repression of antitumor T-helper cell type 1 (Th1) interferon-γ and Th17 T cell responses.

Conclusions. Since different tumor types growing in the same location in the brain share a location-specific phenotype, we suggest that antigen-specific immunotherapies should be based upon expression of both histological type–specific tumor antigens and location-specific antigens. Our findings support clinical application of VSV-TAA therapy with checkpoint inhibition for aggressive brain tumors and highlight the importance of the intracranial microenvironment in sculpting a location-specific profile of tumor antigen expression.

Keywords: cancer immunotherapy, checkpoint inhibitor, glioma, oncolytic virus, vesicular stomatitis virus.

There have recently been highly encouraging advances in the development of effective immunotherapies for the treatment of advanced cancers.[1,2] However, despite significant progress in the fields of prostate cancer[3] and melanoma,[4] clinical application of immunotherapy for poor prognosis primary brain tumors, such as glioblastoma has been less extensively studied. Therefore, significant advances are required to improve our understanding of the immunological profiles of brain tumors and how they are influenced by the unique immune microenvironment maintained within the CNS.[5]

Our previous studies have highlighted the therapeutic potential of immunotherapy using a systemically delivered oncolytic vesicular stomatitis virus (VSV) as a platform for expressing a complementary cDNA library of normal/tumor tissue.[6–10] In particular, we have shown that VSV-cDNA libraries are capable of vaccinating against a wide range of tumor-associated

Received 5 May 2015; accepted 25 July 2015

antigens (TAAs) expressed on tumors of the same histological type as the source of the cDNA library.[6–8] Significantly, efficacy was associated with truly systemic delivery of the VSV-cDNA viruses and was effective at treating murine prostate tumors[6] or subcutaneous (s.c.) B16 tumors,[7] depending upon the source of the cDNA used. In the case of s.c. B16 melanomas, we identified the key TAAs involved in tumor rejection as VSV-expressed neuroblastoma-Ras (N-Ras), cytochrome *c* (Cyt-c), and tyrosinase-related protein 1 (TYRP-1). These VSV-expressed TAAs were therapeutically effective only in combination, not alone, and induced tumor rejection by induction of a T helper cell Th17 antitumor T cell response.[7] We also showed that exactly the same VSV-cDNA library that was effective against s.c. B16 tumors significantly prolonged survival of the same B16 tumors growing intracranially (i.c.).[8] However, while therapy with VSV–N-Ras, VSV–Cyt-C, and VSV–TYRP-1 effectively treated s.c. B16 murine tumors, this combination was completely ineffective against the i.c. B16 tumors.[8] In contrast, immunologic screening of the VSV-cDNA identified a combination of VSV-expressed hypoxia-inducible factor (HIF)–2α, Sox-10, c-Myc, and TYRP-1 as the immunogens against which a Th17 anti i.c. B16 tumor response was therapeutic.[8] These data showed that the immunological profile of tumor antigens expressed by cells of the same histological type is determined by the anatomical location of the tumor.[8] Consistent with this, we demonstrated that the i.c. phenotype of tumor antigen expression was imposed by the unique immune microenvironment within the brain, mediated by the presence of i.c. CD11b+ cells.[8]

These studies raised a critical question related to our ability to develop effective immunotherapies for different types of brain cancers. Thus, if the local brain microenvironment imposes a highly distinct antigenic profile on melanoma tumors growing i.c., would tumors of different histological types also share this profile? If so, this would have profound implications for the treatment of brain tumors of different histological types and may lead to the generation of immunotherapeutic strategies effective against both gliomas, as well as other types of metastatic disease in the brain. Therefore, the aims of the current study were to characterize the immunogenic profile of a variety of cancer types growing in the same i.c. location and to test the hypothesis that immunological targeting of this i.c.-specific phenotype, as opposed to the histological phenotype of a tumor, could lead to an effective treatment for glioma.

We show here that the combination of systemically delivered VSV-expressed HIF-2α, Sox-10, and c-Myc significantly extended survival of mice bearing i.c. GL261 gliomas, just as it was effective against i.c. melanomas (without the need for VSV–TYRP-1). In addition, VSV–HIF-2α, VSV–Sox-10, and VSV–c-Myc therapy against i.c. GL261 tumors was significantly enhanced in vivo by the addition of anti–programmed cell death protein 1 (PD1) antibody alone, or anti-PD1 antibody in combination with anti–cytotoxic T lymphocyte antigen 4 (CTLA4) antibody. Interestingly, the addition of checkpoint inhibitor therapy relieved the suppression of a Th1 antitumor response, which was suppressed in vivo in the absence of anti-PD1 therapy. Taken together, our data support a potential clinical application for VSV-TAA therapy in combination with checkpoint inhibition for aggressive brain tumors such as glioblastoma; they highlight the importance of the i.c. cellular immune environment in maintaining the antigenic/immunogenic identity of brain tumors of different histological types; and they support the concept that effective immunotherapies need to target location-specific tumor phenotypes, as well as the histological tumor phenotypes more traditionally used to characterize immunotherapeutic targets.

Materials and Methods

Cell Lines

Murine B16 cells were grown in Dulbecco's modified Eagle's medium (DMEM; Life Technologies) supplemented with 10% fetal calf serum (FCS) and L-glutamine (Life Technologies). Murine GL261 cells were grown in DMEM supplemented with 10% FCS. Transgenic adenocarcinoma of the mouse prostate (TRAMP-C2 [TC2]) cells, from a prostate tumor in a TRAMP mouse,[11] were routinely grown as tumors in C57BL/6 mice in an androgen-independent manner. K1735 melanoma cells[12] were derived from H-2^k C3H/He mice. The C57BL/6 and C3H mice were purchased from The Jackson Laboratory at 6–8 weeks of age.

Virus

The ASMEL (Altered Self Melanoma Epitope Library) VSV-cDNA library was generated as previously reported.[6–8] Individual viral clones were isolated by limiting dilution as previously described,[7,8] expanded in baby hamster kidney cells, and purified by sucrose gradient centrifugation. VSV–green fluorescent protein (GFP) was manufactured as described.[13]

Tumor Dissociation

Tumors were excised from euthanized mice by local dissection from the brain. Tumors were then dissociated into single-cell suspensions with enzymatic digestion of the extracellular matrix combined with mechanical dissociation using the mouse Tumor Dissociation kit (Miltenyi Biotech) according to the manufacturer's instructions.

HIF-2α Protein in Intracranial Explants and In vitro Cultures

To establish i.c. tumors, 1×10^4 cells in 2 μL phosphate buffered saline (PBS) were stereotactically injected into the brain (1 mm anterior and 2 mm lateral to the bregma) of C57BL/6 (B16, GL261, or TC2 cells) or C3H (K1735 cells) mice. Mice were sacrificed upon sign of distress, and single-cell suspensions of brain tumor explants or in vitro cultured cells (B16, GL261, TC2, or K1735) were plated at 1×10^5 per well. HIF-2α protein expression was measured in cell lysates by enzyme-linked immunosorbent assay (ELISA) (USCN Life Sciences). From in vitro cultures, 1×10^5 cells of each cell line (B16, GL261, TC2, K1735) were also plated and measured for HIF-2α protein.

HIF-2α Protein in Co-cultures of GL261 and Splenic/Brain-Derived CD11b+ Cells

CD11b+ cells were purified from brain-cell suspensions of multiple brains or from the spleens of C57BL/6 mice using CD11b microbeads (Miltenyi Biotech); 1×10^6 CD11b+ cells were co-cultured with (1×10^5) GL261 cells for 24 h, cell-free supernatants were harvested, and HIF-2α protein was measured by ELISA. HIF-2α protein was also evaluated following co-culture of GL261 cells with brain- or spleen-derived CD11b+ cells, in the presence of 10 ng/mL recombinant transforming growth factor (TGF)-β RII Fc Chimera 341-BR (R&D Systems).

Human Tumor Explants

Human primary glioblastoma brain tumor tissue was obtained following surgery. Written informed consent was obtained from all patients in accordance with local institutional ethics review and approval. Within 3 h of resection, explants were dissociated into single-cell suspensions using the human Tumor Dissociation Kit (Miltenyi Biotech) and were depleted of CD11b+ cells using CD11b microbeads. Tumor cells were seeded at 1×10^4 cells ± isolated autologous CD11b+ cells (5×10^3 per well). HIF-2α protein levels were evaluated at 24 h and following 2 weeks of culture. HIF-2α protein was also evaluated from 1×10^3 isolated CD11b+ cells 24 h after explant.

In vivo Studies

All procedures were approved by the Mayo Foundation Institutional Animal Care and Use Committee. To establish i.c. tumors, 1×10^4 GL261 cells in 2 μL PBS were stereotactically injected into the brains of C57BL/6 mice ($n = 7-9$ per group unless otherwise stated, 1 mm anterior and 2 mm lateral to the bregma, using a syringe bearing a 26G needle). Virus, drug, or PBS control (100 μL) was administered intravenously 5 days later and as described.

Over many separate experiments, we have observed that survival of mice with GL261 tumors growing intracranially and treated with nothing at all, PBS, or i.v. injections of VSV-GFP are not significantly different. Therefore, we routinely used either PBS treatment or VSV-GFP as our negative control for these experiments.

For checkpoint inhibition studies, control ChromPure rat immunoglobulin IgG antibody (Jackson Immunochemicals) or anti-PD1 antibody was i.v. injected at 225 μg/mouse/injection (clone RMP 1-14, Bio X Cell) and anti-CTLA4 at 0.1 mg/mouse/injection (Bio X Cell).

In vitro Splenic/Lymph Node T-cell Reactivation and ELISA for Interferon-γ/Interleukin-17

Spleens and lymph nodes were harvested from euthanized mice and dissociated into single-cell suspensions. Red blood cells were lysed with ammonium-chloride-potassium lysis buffer (sterile H_2O containing 0.15 M NH_4Cl, 1.0 mM $KHCO_3$, and 0.1 mM EDTA adjusted to pH 7.2–7.4). Cells were resuspended at 1×10^6 cells/mL in Iscove's modified Dulbecco's medium + 5% FCS + 1% penicillin-streptomycin + 40 μmol/L 2-mercapto-ethanol. Pooled cells (1×10^6 per well) were stimulated with freeze/thaw lysates (equivalent to 1×10^5 cells) of either GL261 tumors recovered from mice bearing i.c. GL261 tumors or in vitro cultured GL261 cells every 24 h for 3 days. Following 48 h culture, cell-free supernatants were assayed by ELISA for interferon (IFN)-γ (BD Biosciences) or interleukin (IL)-17 (R&D Systems). Restimulation was also carried out with splenocytes and lymph node cells depleted of regulatory T cells (Tregs) using CD4+/CD25+ beads (Miltenyi Biotech). Splenocyte and lymph node single-cell isolates were also stimulated as described above with the VSV-N protein derived epitope peptide (VSV-N_{52-59}:RGYVYQG at 5 μg/mL), and supernatants were evaluated for IFN-γ and IL-17.

Statistics

Survival data were analyzed using the log-rank test with GraphPad Prism 6. A 2-sample, unequal variance Student's *t*-test was used to evaluate in vitro data. Statistical significance was determined at $P < .05$.

Results

Intracranial Tumors of Different Histologies Express a Similar HIF-2α^{Hi} Phenotype

Based on our previous studies,[8] we hypothesized that the i.c. microenvironment imposes a HIF-2α^{Hi} phenotype upon different types of tumors, which is distinct from that expressed by the same tumor cells growing in culture. Consistent with this hypothesis, freshly resected i.c. tumors of different histological types, including K1735 melanoma (in C3H mice), as well as B16 melanoma, GL261 glioma, and TC2 prostate cancer (C57BL/6 mice), all expressed a HIF-2α^{Hi} phenotype. In contrast, the same cell lines grown in culture, from which the tumors were initially derived by i.c. implantation, expressed low or undetectable levels of HIF-2α (Fig. 1A). In addition, the HIF-2α^{Hi} phenotype was specific to i.c., as opposed to s.c., tumors (Fig. 1B). Finally, consistent with our identification of a combination of VSV-expressed HIF-2α, Sox-10, c-Myc, and TYRP-1 as the immunogens against which a Th17 anti i.c. B16 tumor response was therapeutic,[8] GL261 tumors growing i.c. expressed a HIF-2α^{Hi}, Sox-10^{Hi}, c-Myc^{Hi} phenotype, which was not expressed by cultured GL261 cells or by GL261 tumors growing in a different, subcutaneous location (Fig. 1C).

CD11b+ Cells in Intact Brain Homogenate Impose a HIF-2α^{Hi} Phenotype on GL261 Cells In vitro in Part Through TGF-β

Previously, we demonstrated that the HIF-2α^{Hi} phenotype of i.c. B16-ova tumors was imposed by brain-associated, but not spleen-derived, CD11b+ cells. In vitro co-culture of GL261cells with CD11b+ cells purified from intact brain homogenate mediated a similar HIF-2α^{Lo} to HIF-2α^{Hi} phenotypic transition (Fig. 2). As for the B16 model, splenic CD11b+ cells were unable to impose a HIF-2α^{Hi} phenotype on in vitro cultured glioma cells (Fig. 2). While neutralization of neither

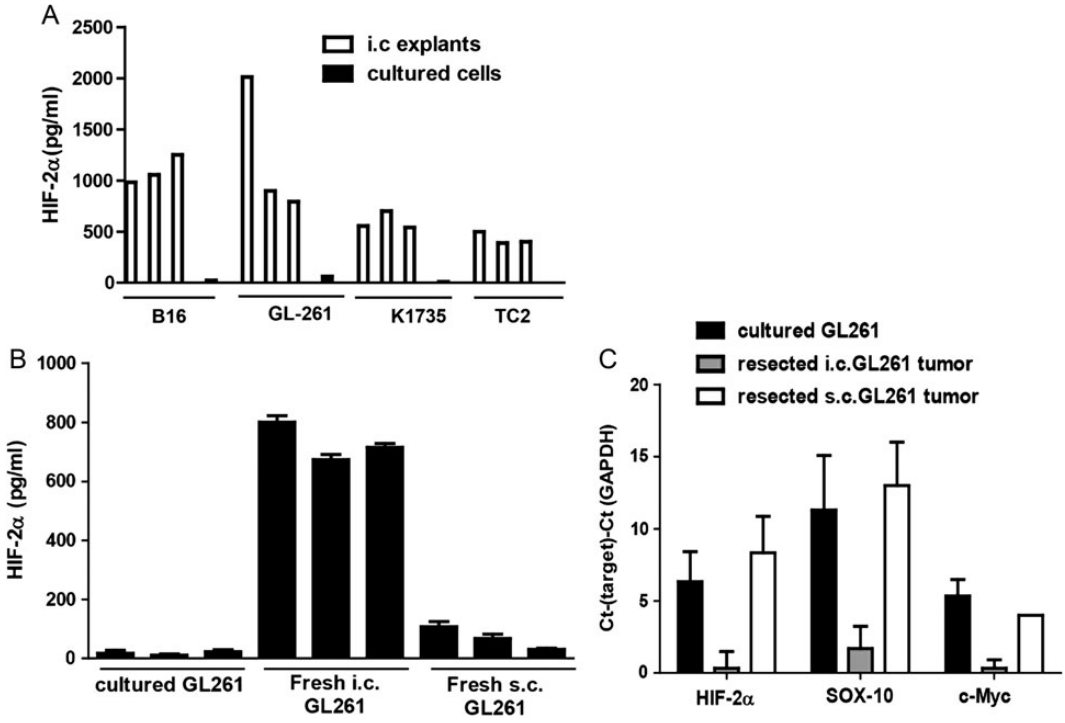

Fig. 1. Intracranial tumors of different histology express a HIF-2α^{Hi} phenotype. (A) Tumors established in the brains of C57BL/6 (B16, GL261, or TC2 cells) or C3H (K1735) mice were dissected upon sacrifice (tumor explants), and tumor cells were seeded at 1×10^5 per well. Of each cell line, 1×10^5 cells cultured in vitro (cultured) were also plated. HIF-2α was measured by ELISA after 24 h. Error bars are expressed as SD. (B) HIF-2α protein expression from GL261 cells either grown in culture (3 plates) or freshly resected from i.c. tumors ($n = 3$) or from s.c. GL261 tumors was measured by ELISA with samples standardized for equal protein loading. (C) cDNA from GL261 cells either grown in culture (3 plates) or freshly resected from i.c. tumors ($n = 3$) or from s.c. GL261 tumors was screened by quantitative real-time PCR for expression of HIF-2α, Sox-10, and c-Myc. The difference in cycle threshold (Ct) for expression of the target gene to that of the control glyceraldehyde 3-phosphate dehydrogenase (GAPDH) gene (Ct(Target) − Ct(GAPDH)) is shown. Results are representative of 2 separate experiments.

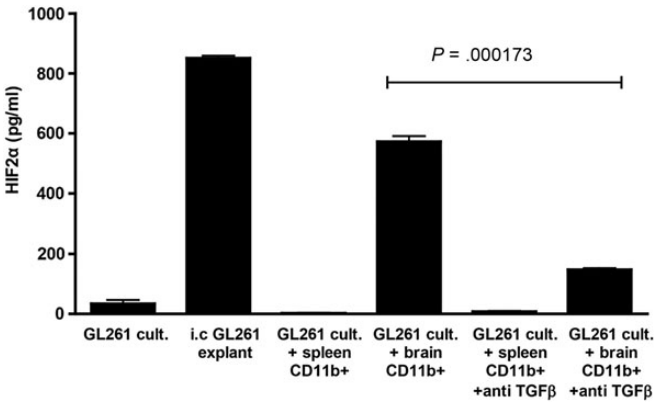

Fig. 2. Brain-derived CD11b+ cells impose a HIF-2α^{Hi} phenotype on in vitro cultured GL261, in part through TGF-β. HIF-2α expression was measured by ELISA from: 1×10^5 GL261 cells cultured in vitro for 24 h; GL261 i.c. tumors, dissected from the brain upon sacrifice and plated at 1×10^5 cells per well for 24 h; 1×10^5 GL261 cells co-cultured for 24 h with 1×10^6 CD11b+ cells purified from normal splenocytes of C57BL/6 mice; 1×10^5 GL261 cells co-cultured for 24 h with 1×10^6 CD11b+ cells purified from normal brains of C57BL/6 mice. Cultures with added CD11b+ cells (spleen- or brain-derived) were repeated in the presence of recombinant TGF-β RII Fc Chimera at 10 ng/mL. Results are representative of 3 separate measurements. Error bars are expressed as SD. *$P = .000173$, between the groups as indicated.

tumor necrosis factor−α, vascular endothelial growth factor, nor IFN-γ prevented induction of the HIF-2α^{Hi} phenotype in GL261 and brain-associated CD11b+ cell co-cultures (data not shown), blocking TGF-β significantly reduced HIF-2α expression ($P = .000173$) (Fig. 2).

Human Tumor Explants Express a HIF-2α^{Hi} Phenotype That Is Reduced Over Time

To investigate how the murine model might reflect the patient situation, we studied the HIF-2α phenotype of primary human brain tumor samples. Freshly resected tumors cultured with their own autologous CD11b+ cells exhibited a HIF-2α^{Hi} phenotype, although levels of HIF-2α were consistently lower than in resected murine tumors (Fig. 3). Brain tumor explants depleted of CD11b+ cells expressed lower levels of HIF-2α after 24 h of culture, although this did not reach statistical significance ($P = .101$) (Fig. 3). The CD11b+ cells themselves did not express significant levels of HIF-2α (Fig. 3). After 2 weeks, CD11b+ cells within these co-cultures were lost, and the level of tumor cell–associated HIF-2α was significantly reduced compared with levels seen at 24 h post explant ($P = .017$) (Fig. 3). Therefore, human brain tumors also express a HIF-2α^{Hi} phenotype which is maintained, at least in part, by immune cells within the brain microenvironment.

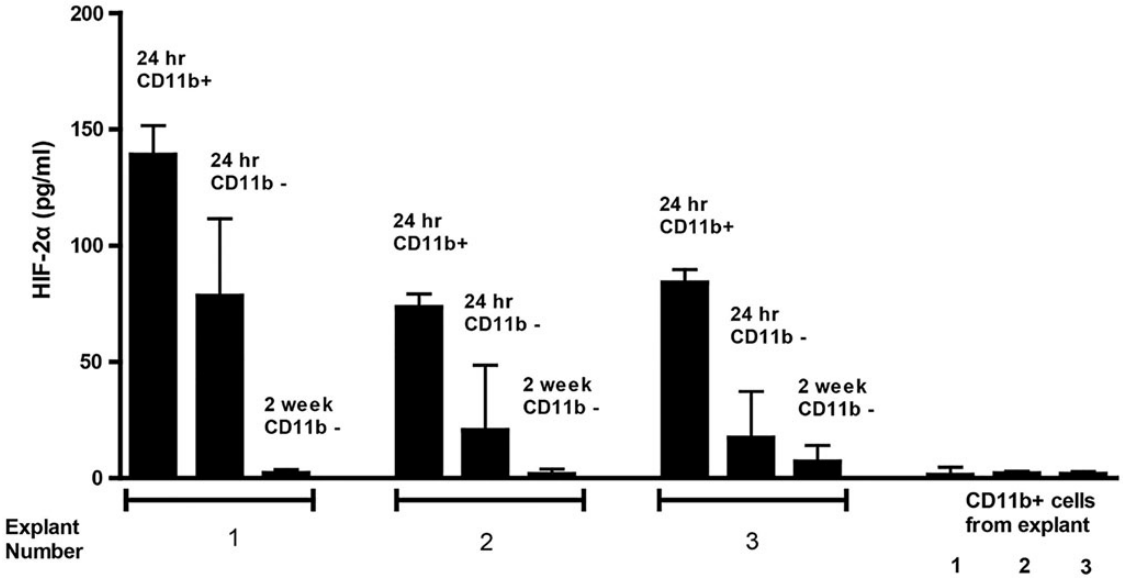

Fig. 3. Human brain tumor explants express a HIF-2α^{Hi} phenotype which diminishes with time. Human brain tumor explants were recovered from surgery and depleted of CD11b+ cells. Tumor cells were plated at 1×10^4 per well either alone (24 h CD11b−) or with 5×10^3 CD11b+ cells (24 h CD11b+). HIF-2α expression was measured at 24 h. In cultures from which tumor cells survived more than a week, HIF-2α was measured from 1×10^4 tumor cells after 2 weeks, by which time CD11b+ cells had been washed away/died (2 wk CD11b-). HIF-2α was also measured from 1×10^3 separated CD11b+ cells 24 h after explant. Results are representative of 3 separate measurements. Error bars are expressed as SD.

Intracranial GL261 Can Be Treated With VSV-Tumor–Associated Antigen Therapy and Enhanced by Addition of Checkpoint Inhibitors

We showed previously that although mice bearing s.c. B16 tumors were treated successfully with a combination of VSV-expressed N-Ras, Cyt-c, and TYRP-1, i.c. B16 tumors were successfully treated only with a combination of VSV-expressed HIF-2α, Sox-10, c-Myc, and TYRP-1.[7,8] Therefore, we tested the hypothesis that effective immunotherapy of an i.c. tumor of a different histological type could be targeted against this common i.c. tumor phenotype imposed by the brain microenvironment. Consistent with this, systemic delivery of VSV-expressed HIF-2α, Sox-10, and c-Myc generated significant therapy over control treatment ($P = .0001$) (Fig. 4A). Although a combination of just 2 of the VSV-TAAs gave significant therapy compared with control treatment ($P = .0001$), optimal therapy required the combination of all 3 antigens (HIF-2α, Sox-10, c-Myc) ([VSV–HIF-2α/Sox-10/c-Myc] vs [VSV–HIF-2α/Sox-10 + VSV-GFP], $P = .0414$). Unlike in the B16 i.c. model, addition of the VSV–TYRP-1 virus gave no added therapeutic benefit to treatment with VSV-expressed HIF-2α, Sox-10, and c-Myc (data not shown). Consistent with our previous data with B16 i.c., as opposed to s.c. tumors, the combination of VSV-expressed N-Ras, Cyt-c, and TYRP-1 was ineffective against i.c. GL261 tumors and offered no significant therapeutic advantage over control therapy ($P = .1432$) (Fig. 4A).

Next, we investigated whether the viroimmunotherapy associated with VSV-TAA therapy of i.c. GL261 could be enhanced through combination with immune checkpoint inhibition.[2,14] To do this, mice bearing i.c. GL261 tumors were treated with fewer i.v. systemic injections of VSV-expressed HIF-2α, Sox-10, and c-Myc (9 instead of the 12 of Fig. 4A) so that any additional therapeutic value of combination with the checkpoint inhibitor antibody anti-PD1 could be detected. Addition of anti-PD1 antibody significantly extended survival compared with the virus combination alone ($P = .0006$) (Fig. 4B). In these experiments, anti-PD1 antibody treatment was initiated on day 13, only shortly before mice not treated with VSV combinations started to die (day 15) (Fig. 4B). Therefore, it is likely that the lack of efficacy of anti-PD1 therapy alone that is seen in the current protocol is due to late initiation of checkpoint inhibition and that earlier monotherapy regimens may be more effective.

Anti-PD1 Antibody Uncovers a Th1 Response Against Intracranial GL261

We showed previously that the therapeutic antitumor response to self-TAA induced by VSV-cDNA library treatment is mediated by Th17 CD4+ T cells, and no Th1 IFN-γ T cell responses could be detected.[6–8] As expected, therefore, mixed splenocytes and lymph node cultures from mice bearing i.c. GL261 tumors following treatment with VSV-TAA (HIF-2α, Sox-10, c-Myc) did not secrete IFN-γ in response to challenge with freeze/thaw lysates of explanted i.c. GL261 tumors (Fig. 5A). In contrast, similar mixed cultures from mice treated with the same VSV-TAA + anti-PD1 antibody secreted significant levels of IFN-γ ($P = .0104$), suggesting that checkpoint inhibition through the PD1 axis uncovered a Th1 response to poorly immunogenic self-antigens (Fig. 5A). Consistent with the distinct antigenic nature of GL261 cells growing in situ in the brain compared with the same cells growing in culture (Figs 1 and 2), splenocyte and lymph node cultures from mice treated with VSV–HIF-2α/Sox-10/c-Myc + anti-PD1 did not secrete IFN-γ in response to challenge with freeze/thaw lysates derived from GL261 cells cultured in vitro (Fig. 5B). These data suggest that a Th1 response to a unique antigenic profile

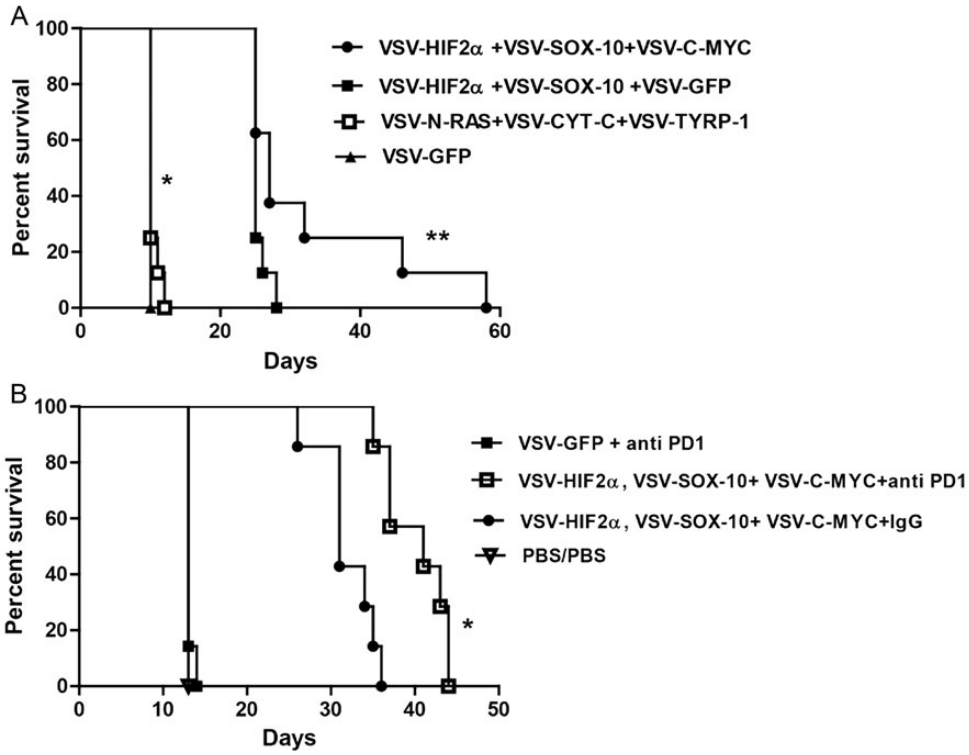

Fig. 4. VSV-TAA therapy of intracranial GL261 tumors with checkpoint inhibition. (A) C57BL/6 mice bearing 5-day established i.c. GL261 tumors were treated intravenously ($n = 7–8$ mice per group) with a total of 5×10^6 plaque-forming units (pfu) of VSV-HIF-2α, VSV-Sox-10, and VSV-c-Myc; VSV-HIF-2α, VSV-Sox-10, and VSV-GFP; VSV-N-Ras, VSV-Cyt-c, and VSV-TYRP-1; or VSV-GFP on days 6, 8, and 10; 13, 15, and 17; 20, 22, and 24; and 27, 29, and 31, respectively. Survival with time is shown. Representative of 3 separate experiments. *$P = .0001$ between VSV-HIF-2α, VSV-Sox-10, and VSV-c-Myc and VSV-GFP, and **$P = .0414$ between VSV-HIF-2α, VSV-Sox-10, VSV-c-Myc and VSV-HIF-2α, VSV-Sox-10+, VSV-GFP. (B) C57BL/6 mice bearing 5-day established i.c. GL261 tumors were treated intravenously ($n = 7–8$ mice per group) with a total of 5×10^6 pfu of VSV-GFP; VSV-HIF-2α, VSV-Sox-10, and VSV-c-Myc, or PBS on days 6, 8, and 10; 13, 15, and 17; and 20, 22, and 24, respectively. On days 13, 15, and 17 and 20, 22, and 24 these groups were treated intravenously with either PBS, control IgG antibody, or anti-PD1 antibody at 10 mg/kg/mouse as shown. Survival with time is shown. Representative of 2 separate experiments. *$P = .0006$ between VSV + anti-PD1 combination and VSV combination alone.

associated with i.c. GL261 tumors is generated following VSV-TAA viroimmunotherapy but that it is suppressed in vivo and can be de-repressed upon checkpoint inhibition.

Anti-PD1 Antibody Therapy Does Not Enhance the Th17 Response Against Intracranial GL261

Interestingly, despite enhancing therapeutic efficacy in vivo (Fig. 4B), checkpoint inhibition with anti-PD1 did not significantly enhance the Th17 response generated by VSV–HIF-2α/Sox-10/c-Myc treatment ($P = .674$) (against either i.c. explanted or cultured GL261 freeze/thaw lysates) (Fig. 5C and D). Both Th1 IFN-γ and Th17 anti-i.c. GL261 responses were induced by only VSV-TAA, as opposed to VSV-GFP (Fig. 5A and C, respectively), indicating that virally mediated expression of tumor antigens was required for an effective immune response.

Anti-PD1 Antibody Enhances the Th1 Response Against VSV

As we reported previously,[8] VSV-TAA treatment reproducibly induced a Th1 response against VSV antigens (Fig. 5E). This anti-VSV Th1 response was also significantly enhanced in mice treated with checkpoint inhibition compared with VSV-TAA treatment alone ($P = .00375$) (Fig. 5E).

Anti-PD1 Checkpoint Inhibition Mimics Depletion of Tregs

As before (Fig. 5A), the addition of anti-PD1 to VSV-TAA therapy uncovered an antitumor Th1 response (Supplementary Fig. SA, lanes 1/2 compared with 3/4). In vitro depletion of Tregs from the mixed splenocyte/lymph node cultures prior to restimulation with freeze/thaw lysates also de-repressed the Th1 IFN-γ T cell response against i.c. GL261, compared with Treg-intact cultures (Supplementary Fig. SA, lanes 1/2 compared with 5/6). However, Treg depletion from splenocyte/lymph node cultures of mice treated with VSV-TAA + anti-PD1 did not further enhance the Th1 IFN-γ T cell response already uncovered by anti-PD1 therapy (Supplementary Fig. SA, lanes 3/4 compared with 7/8). Neither anti-PD1 nor in vitro Treg depletion enhanced IL-17 responses generated by VSV-TAA therapy (Supplementary Fig. SB).

These data suggest that anti-PD1 immune checkpoint inhibition may operate in vivo, to de-repress an antitumor Th1 IFN-γ T cell response and that this may be effected, at least in part, by affecting Treg function. Experiments are currently

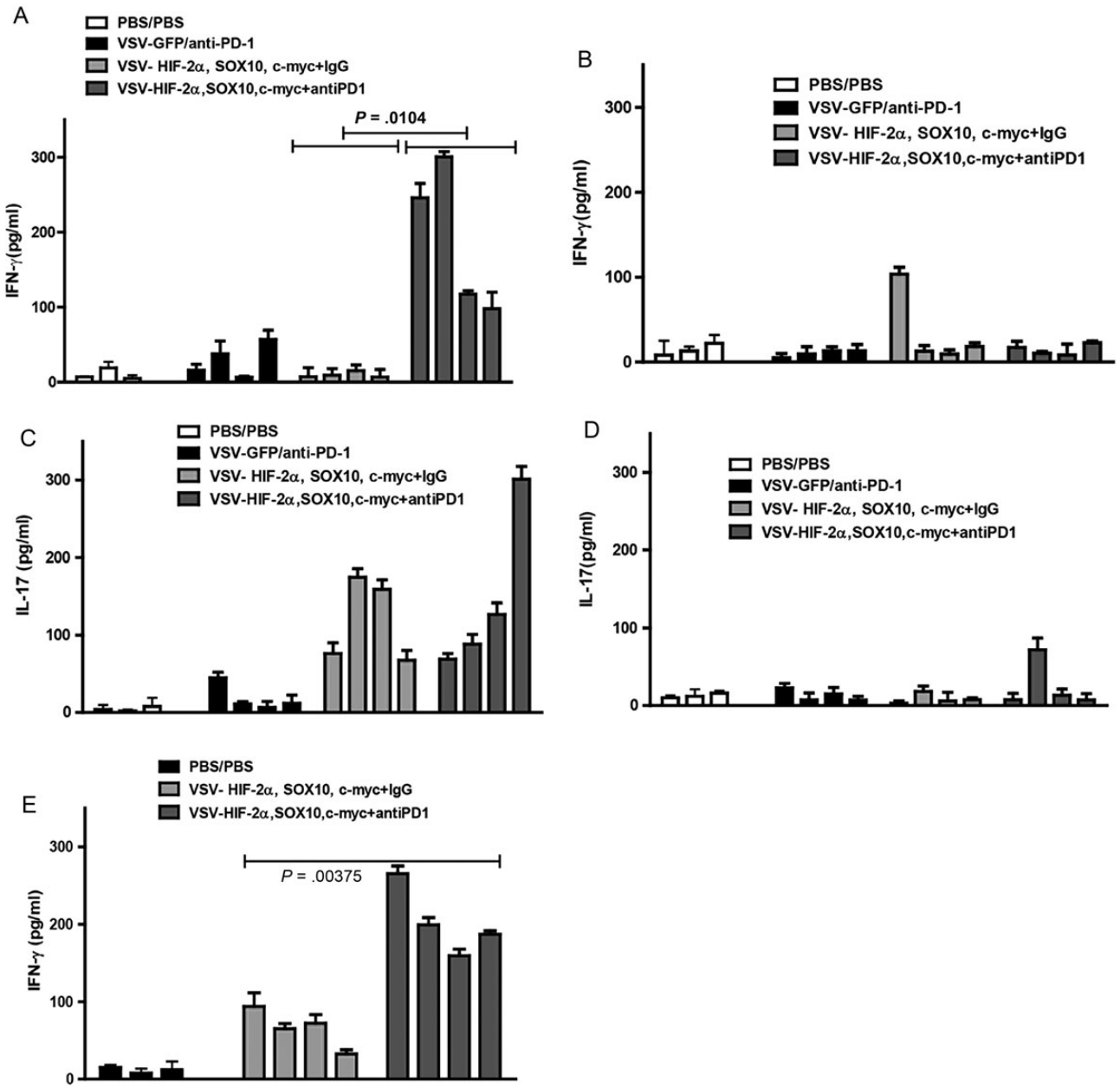

Fig. 5. Checkpoint inhibition uncovers a Th1 immune response against tumor. (A–D) Splenocytes and lymph nodes were pooled from 3 C57BL/6 mice per group bearing 5-day established i.c. GL261 tumors treated with either PBS/PBS; VSV-GFP + anti-PD1 antibody; VSV-HIF-2α, VSV-Sox-10, and VSV-c-Myc + IgG; or VSV-HIF-2α, VSV-Sox-10, and VSV-c-Myc + anti-PD1 antibody. Cells were plated at 1×10^6 cells per well and restimulated in vitro 3 times at 24-h intervals with 1×10^5 cells of freeze/thaw lysates of GL261 tumors recovered from mice bearing i.c. GL261 tumors (A and C) or with freeze/thaw lysates of in vitro cultured GL261 (B and D). Forty-eight hours later, supernatants were assayed for IFN-γ (A and B) or IL-17 (C and D) by ELISA. (E) Splenocytes and lymph nodes were also restimulated with the VSV–N protein derived epitope at 5 μg/mL, 3 times for 24 h. Forty-eight hours later, supernatants were assayed for IFN-γ. Each result is representative of 3 separate measurements. Error bars are expressed as SD.

under way to investigate the effects of anti-PD1 therapy on Treg numbers and function in the context of VSV-TAA therapy.

Combination Checkpoint Inhibition Further Improves VSV-TAA Therapy

Given our success with enhancing VSV-TAA therapy with single checkpoint inhibitor therapy, we tested a combination of anti-PD1 and anti-CTLA4 checkpoint inhibition to target separate stages of the T cell activation/repression pathway,[15] in combination with VSV-TAA therapy. Importantly, this combination checkpoint inhibitor approach reflects current clinical trial activity (https://clinicaltrials.gov/ct2/show/NCT02017717). As before, anti-PD1 treatment once again gave a significant improvement in survival in combination with VSV-TAA therapy (Fig. 6A) in mice treated with a suboptimal dose of 6 injections

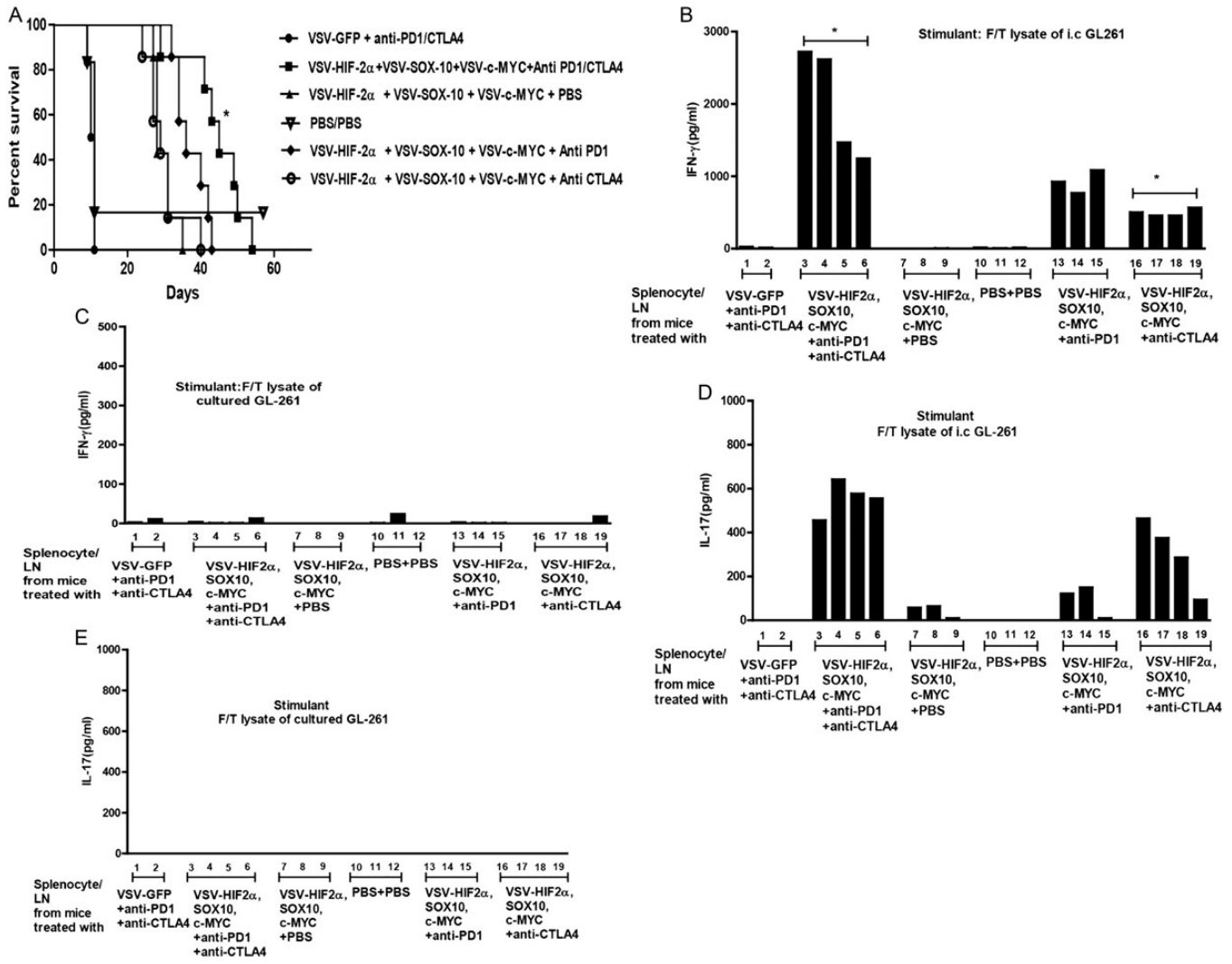

Fig. 6. Double checkpoint inhibition therapy enhances treatment with VSV-TAA. (A) C57BL/6 mice bearing 5-day established i.c. GL261 tumors were treated intravenously ($n = 7–8$ mice per group) with a total dose of 5×10^6 pfu of VSV-GFP; VSV-HIF-2α, VSV-Sox-10, and VSV-c-Myc, or PBS on days 6, 8, and 10 and 13, 15, and 17, respectively. On days 13, 15, and 17 these groups were also treated with either anti-PD1 antibody, anti-CTLA4 antibody, anti-PD1 antibody + anti-CTLA4 antibody, or PBS as shown. Survival with time is shown. Representative of 2 separate experiments. *$P = .0015$ between VSV-HIF-2α, VSV-Sox-10, and VSV-c-Myc and VSV–HIF-2α, VSV–Sox-10, and VSV–c-Myc + anti-PD1 and anti-CTLA4. (B–E) Splenocytes and lymph nodes were pooled from 3 C57BL/6 mice per group bearing 5-day established i.c. GL261 tumors treated with either VSV-GFP + anti-PD1 + anti-CTLA4; VSV–HIF-2α, VSV–Sox-10, and VSV–c-Myc + anti-PD1 antibody + anti-CTLA4 antibody; VSV–HIF-2α, VSV–Sox-10, and VSV–c-Myc + PBS; PBS + PBS; VSV–HIF-2α, VSV–Sox-10, and VSV–c-Myc + anti-PD1 antibody; or VSV–HIF-2α, VSV–Sox-10, and VSV–c-Myc + anti-CTLA4 antibody. Cells were plated at 1×10^6 cells per well and restimulated in vitro 3 times at 24-h intervals with 1×10^5 cells of freeze/thaw lysates of GL261 tumors recovered from mice bearing i.c. GL261 tumors (B and D) or with freeze/thaw lysates of in vitro cultured GL261 (C and E). Forty-eight hours later, supernatants were assayed for IFN-γ (B and C) or IL-17 (D and E) by ELISA. (B) *$P = .0282$ comparing lanes 3–6 and 16–19.

of VSV-TAA (as opposed to the 12 of Fig. 4A and the 9 of Fig. 4B). In contrast, anti-CTLA4 as a monosupportive therapy for VSV-TAA gave no added therapeutic benefit to VSV-TAA alone (Fig. 6A). However, when used together, anti-PD1 and anti-CTLA4 significantly improved VSV-TAA therapy alone ($P = .0015$), and the combination was also more effective than VSV-TAA + anti-PD1 ($P = .0184$) or VSV-TAA + anti-CTLA4 ($P = .0016$) alone.

As before (Fig. 4), addition of anti-PD1 therapy to VSV-TAA uncovered a Th1 IFN-γ T cell response to i.c. GL261 explants that was not detected from mice treated with VSV-TAA alone (Fig. 6B). This was also true of anti-CTLA4 therapy in combination with VSV-TAA, although to a lesser extent than with anti-PD1 (Fig. 6B). However, splenocyte/lymph node cultures from mice treated with VSV-TAA and both anti-PD1 and anti-CTLA4 checkpoint inhibition displayed enhanced Th1 IFN-γ T cell response against i.c. GL261 compared with VSV-TAA therapy in combination with either checkpoint inhibitor alone, although this only reached statistical significance when compared with the anti-CTLA4 treatment group ($P = .0282$) (Fig. 6B).

With respect to the Th17 recall response, VSV-TAA therapy in combination with anti-CTLA4 showed a strong trend to enhancing the Th17 response to i.c. GL261 responses (Fig. 6D) compared with VSV-TAA therapy alone or in combination with anti-PD1. Interestingly, splenocyte/lymph node cultures from mice treated with VSV-TAA combined with both anti-CTLA4 and anti-PD1 therapy generated the strongest Th17 recall responses against i.c GL261 (Fig. 6D). In contrast, no significant secretion of IFN-γ or IL-17 was detected in response to challenge with lysates of cultured GL261 cells (Fig. 6C and E).

Taken together, these data show that addition of checkpoint inhibitors, either singly or in combination, can enhance therapeutic responses to VSV-TAA treatment and that these increases in therapy are associated with the de-repression of an antitumor Th1 IFN-γ T cell response (anti-PD1, anti-CTLA4, or both) and of the antitumor Th17 response (anti-PD1 + anti-CTLA4).

Discussion

We show here that different histological types of tumor growing intracranially all expressed a similar location-specific HIF-2α^{Hi} phenotype, distinct from the phenotype of the same tumor cells in culture, or, at least in the case of B16, tumors at different locations in vivo.[8] Critically, this was also true of freshly resected human brain tumor explants. This allowed us to use viroimmunotherapy, initially identified as effective against melanoma growing intracranially, against a histologically separate glioma. This therapy was significantly enhanced by further combination with checkpoint inhibition, which appeared to mimic Treg depletion by de-repressing a Th1 IFN-γ antitumor T cell response.

Malignant primary brain tumors are associated with devastating survival outcomes.[16] In this respect, we show here that i.c. derived tumors of different histologies (prostate cancer, melanoma, and glioma) all express high levels of HIF-2α compared with their in vitro cultured counterparts (Fig. 1). Brain-derived, but not splenic-derived, CD11b+ cells imposed the HIF-2α^{Hi} phenotype on GL261 cells cultured in vitro, mediated in part by TGF-β (Fig. 2). Significantly, we also verified that freshly resected human brain tumor explants expressed a HIF-2α^{Hi} phenotype, which diminished with time, and that this phenotype appeared to be maintained in part by human brain tissue–derived CD11b+ cells (Fig. 3). Experiments are currently under way to determine more precisely the phenotype of these CD11b+ cells as microglia, macrophages, or other cell types.

Based on these results, we tested the hypothesis that the i.c.-specific HIF-2α^{Hi} phenotype, which we initially characterized to be imposed upon B16 melanomas growing i.c.,[8] could also be targeted to treat the GL261 glioma. Therefore, we evaluated the efficacy of treatment with VSV expressing the antigens HIF-2α, Sox-10, and c-Myc, which we previously showed to confer treatment against i.c. B16-ova tumors.[8] Systemic delivery of VSV–HIF-2α, VSV–Sox-10, and VSV–c-Myc significantly improved therapy compared with treatment with VSV-GFP or VSV expressing only 2 antigens from the signature (Fig. 4). Mice treated with the antigenic signature (VSV–N-Ras, VSV–Cyt-c, and VSV–TYRP-1) shown to be effective against s.c. located B16 tumors[8] demonstrated no therapeutic advantage over controls (VSV-GFP). These data clearly demonstrate the importance of the anatomical location of the tumor when considering the profile of TAA to be targeted by immunotherapy (Fig. 4).

Given the success of antibodies used to target the T cell inhibitory factors CTLA4, PD1, and its ligand PDL1 in cancer immunotherapies,[2,14,17,18] we evaluated the therapeutic response of VSV-TAA in combination with checkpoint inhibition. Addition of anti-PD1 antibody to the VSV–HIF-2α, VSV–Sox-10, and VSV–c-Myc combination enhanced therapy (Figs 4B and 6A), while addition of anti-CTLA4 antibody did not provide any therapeutic benefit (Fig. 6A). Nonetheless, triple therapy of VSV–HIF-2α, VSV–Sox-10, and VSV–c-Myc with anti-PD1 and anti-CTLA4 antibodies generated the most effective therapy compared with the VSV signature alone or in combination with either single checkpoint inhibitor (Fig. 6A).

Memory recall responses were observed only following restimulation in vitro with freeze/thaw lysates from i.c. derived GL261 explants, but not from in vitro cultured GL261 cells (Figs 4 and 6). These results confirm that the immune responses induced by VSV-TAA treatment were to the unique antigenic signature imposed intracranially (Fig. 5), which is clearly distinct from the immunogenic profile of the cells growing under other conditions. Cotreatment with anti-PD1 antibody uncovered a Th1 response to the i.c. tumor, which was previously not detectable following treatment with the VSV-cDNA library alone[8] (Fig. 5A). However, anti-PD1 therapy did not enhance the Th17 response against i.c. GL261 (Fig. 5C). Anti-PD1 treatment also significantly enhanced the antivirus IFN-γ dependent Th1 response (Fig. 5E), which might be expected to lead to more rapid clearance of virus following any of the later i.v. treatments. Indeed, this may help to explain why we observe that multiple, repeated injections of virus are required for full therapeutic benefit.[6–8]

De-repression of an antitumor IFN-γ dependent Th1 response was also observed by depleting Tregs from in vitro splenocyte/lymph node cultures (Supplementary Fig. S). Since both Treg depletion and anti-PD1 immune checkpoint inhibition had similar effects in uncovering this antitumor Th1 IFN-γ T cell response, it may be that anti-PD1 therapy in combination with VSV-TAA directly, or indirectly, affects Treg function. Experiments are currently under way to investigate the effects of anti-PD1 therapy on Treg numbers and function in the context of VSV-TAA therapy.

Our data here are significant in several different and important respects. In the first, we show that different tumor types growing in the same location in the brain share a location-specific phenotype between histological types of tumor. This phenotype is also significantly different from the phenotype of the tumor cells that would be predicted from analysis of those cells growing in vitro, or at other anatomical locations. Thus, common immunogens may be targeted to treat brain tumors of different histological types, even though those different histologies may not necessarily share antigen expression when analyzed in vitro or from other primary tumor sites.

Second, we demonstrate that this location-specific i.c. phenotype is mediated by CD11b+ cells of the brain microenvironment in our murine model. Our data from freshly resected human tumor explants also suggest that CD11b+ cells are important in imposing this location-specific i.c. phenotype, although further experiments are required to confirm the concordance of the

murine and human data. Importantly, the phenotype becomes transient when tumor cells are studied outside of the context of their i.c. growth and the presence of brain-derived CD11b+ cells. Therefore, anti-glioma immunotherapies need to be developed based upon expression of both histological type–specific tumor antigens and location-specific antigens. These results argue strongly for the analysis of human tumor antigen expression profiles from samples recovered as quickly, or maintained long term as orthotopically, as possible.[19]

Third, we show here, for the first time to our knowledge, that glioma can be treated systemically with a combination of VSV expressing 3 different TAAs. This VSV-TAA immunotherapy was significantly enhanced by combination with 2 checkpoint inhibitors, associated with de-repression of an antitumor Th1 IFN-γ T cell response (anti-PD1, anti-CTLA4, or both) and of the antitumor Th17 response (anti-PD1 + anti-CTLA4).

In summary, VSV-TAA therapy of i.c. GL261 glioma was improved by addition of checkpoint inhibition, supporting clinical application of oncolytic virotherapy with immunomodulatory agents[2,18,20,21] as a novel therapeutic approach for poor prognosis brain tumors. Furthermore, we emphasize the importance of the anatomical location of the tumor when considering the profile of tumor antigens to be targeted by immunotherapy and show that the distinct local cellular immune microenvironment of the brain plays a key role in imposing, and maintaining, tumor antigen expression. These data will lead to design of novel, location-specific immunotherapies against clinically challenging intracranial tumors.

Supplementary Material

Supplementary material is available at *Neuro-Oncology Journal* online (http://neuro-oncology.oxfordjournals.org/).

Funding

This work was supported by NIH grants R01 CA175386-01 and RO1 1CA08961-03, the European Research Council, the University of Minnesota/Mayo Partnership, the Schulze Family Foundation, the Paul Family, SPORE funding CA108961, SPORE IR 09-00315, the University of Leeds, and the Mayo Foundation. We also wish to acknowledge support from Yorkshire Cancer Research and Children with Cancer UK.

Acknowledgments

We thank Toni Higgins for expert secretarial assistance.

Conflict of interest statement. None declared.

References

1. Vanneman M, Dranoff G. Combining immunotherapy and targeted therapies in cancer treatment. *Nat Rev Cancer*. 2012;12(4):237–251.
2. Lichty BD, Breitbach CJ, Stojdl DF, Bell JC. Going viral with cancer immunotherapy. *Nat Rev Cancer*. 2014;14(8):559–567.
3. Kantoff PW, Higano CS, Shore ND, et al. Sipuleucel-T immunotherapy for castration-resistant prostate cancer. *New Engl J Med*. 2010;363(5):411–422.
4. Hodi FS, O'Day SJ, McDermott DF, et al. Improved survival with ipilimumab in patients with metastatic melanoma. *New Engl J Med*. 2010;363(8):711–723.
5. Fecci PE, Heimberger AB, Sampson JH. Immunotherapy for primary brain tumors: no longer a matter of privilege. *Clin Cancer Res*. 2014;20(22):5620–5629.
6. Kottke T, Errington F, Pulido J, et al. Broad antigenic coverage induced by viral cDNA library-based vaccination cures established tumors. *Nature Med*. 2011;2011:854–859.
7. Pulido J, Kottke T, Thompson J, et al. Using virally expressed melanoma cDNA libraries to identify tumor-associated antigens that cure melanoma. *Nat Biotechnol*. 2012;30(4):337–343.
8. Alonso-Camino V, Rajani K, Kottke T, et al. The profile of tumor antigens which can be targeted by immunotherapy depends upon the tumor's anatomical site. *Mol Ther*. 2014;22:1936–1948.
9. Boisgerault N, Kottke T, Pulido J, et al. Functional cloning of recurrence-specific antigens identifies molecular targets to treat tumor relapse. *Mol Ther*. 2013;21(8):1507–1516.
10. Zaidi S, Blanchard M, Shim K, et al. Mutated BRAF emerges as a major effector of recurrence in a murine melanoma model after treatment with immunomodulatory agents. *Mol Ther*. 2015; 23(5):845–856.
11. Kottke T, Sanchez-Perez L, Diaz RM, et al. Induction of hsp70-mediated, Th17 autoimmunity can be exploited as immunotherapy for metastatic prostate cancer. *Cancer Res*. 2007;67:11970–11979.
12. Chong H, Hutchinson G, Hart IR, Vile RG. Expression of costimulatory molecules by tumor cells decreases tumorigenicity but may also reduce systemic anti-tumor immunity. *Hum Gene Ther*. 1996;7:1771–1779.
13. Fernandez M, Porosnicu M, Markovic D, Barber GN. Genetically engineered vesicular stomatitis virus in gene therapy: application for treatment of malignant disease. *J Virol*. 2002;76(2):895–904.
14. Pardoll DM. The blockade of immune checkpoints in cancer immunotherapy. *Nat Rev Cancer*. 2012;12(4):252–264.
15. Shin DS, Ribas A. The evolution of checkpoint blockade as a cancer therapy: what's here, what's next? *Curr Opin Immunol*. 2015;33C:23–35.
16. Johnson DR, O'Neill BP. Glioblastoma survival in the United States before and during the temozolomide era. *J Neurooncol*. 2012;107(2):359–364.
17. Quezada SA, Peggs KS. Exploiting CTLA-4, PD-1 and PD-L1 to reactivate the host immune response against cancer. *Br J Cancer*. 2013;108(8):1560–1565.
18. Engeland CE, Grossardt C, Veinalde R, et al. CTLA-4 and PD-L1 checkpoint blockade enhances oncolytic measles virus therapy. *Mol Ther*. 2014;22(11):1949–1959.
19. Sarkaria JN, Carlson BL, Schroeder MA, et al. Use of an orthotopic xenograft model for assessing the effect of epidermal growth factor receptor amplification on glioblastoma radiation response. *Clin Cancer Res*. 2006;12(7 Pt 1):2264–2271.
20. Elsedawy NB, Russell SJ. Oncolytic vaccines. *Expert Rev Vaccines*. 2013;12(10):1155–1172.
21. Andtbacka RHI, Kaufman HL, Collichio F, et al. Talimogene laherparepvec improves durable response rate in patients with advanced melanoma. *J Clin Oncol*. 2015; doi: 10.1200/JCO.2014.58.3377. [Epub ahead of print].